02

Determination of conductivity electron concentration in single-crystalline n-GaSb samples using FIR reflection spectra at $T = 295$ K

© A.G. Belov[1], E.V. Molodtsova[1], S.S. Kormilitsina[1,2], R.Yu. Kozlov[1,2], E.O. Zhuravlev[1,2], S.A. Klimin[3], N.N. Novikova[3], V.A. Yakovlev[3]

[1] State Research and Planning Institute for the Rare Metal Industry (JSC „Giredmet"), 111524 Moscow, Russia
[2] National Research University of Technology „MISIS" (NITU MISIS), 119049 Moscow, Russia
[3] Institute of Spectroscopy of RAS (ISAS), 108840 Troitsk, Moscow, Russia
e-mail: klimin@isan.troitsk.ru

Received November 11, 2022
Revised March 01, 2023
Accepted May 31, 2023

A method is proposed for separately determining the concentrations of „light" and „heavy" electrons in *n*-GaSb. It is based on the analysis of reflection spectra in the far infrared region, taking into account the plasmon-phonon coupling. Calibration curves have been calculated that allow one to determine the concentrations of „light" and „heavy" electrons in GaSb using the frequency of high-energy coupled plasmon-phonon mode. For a series of *n*-GaSb samples the reflection spectra were measured and the concentrations of „light" and „heavy" electrons were determined at room temperature. Electrophysical Van der Paw measurements have been performed on the same samples at room temperature. By comparing the optical and Hall data, the ratios of the mobilities of „light" and „heavy"electrons (parameter b) were determined. This method of determining the value of the parameter b is used for the first time.

Keywords: *n*-GaSb, reflection spectra, plasmon-phonon coupling, Van der Paw method, „light" and „heavy" electrons.

DOI: 10.61011/EOS.2023.07.57129.4318-23

Introduction

This paper is a continuation of the studies carried out at JSC „Giredmet" for a number of years, with the goal of developing non-contact and non-destructive methods for monitoring of free charge carriers concentration (FCCC) in various semiconductor materials [1–3]. These studies are based on a method for determining the FCCC, based on an analysis of the spectral dependences of the reflectance. The measured reflectance spectra are processed using dispersion analysis to determine the dielectric constant ε and obtain the characteristic wave number. Next, the value of FCCC is calculated using the calculated calibration dependence. Although all measurements were performed at room temperature, the approach under consideration is quite suitable for analyzing the reflectance spectra of samples at low temperatures.

Standard measurements of resistivity and Hall coefficient give good results in determining the FCCC and mobility. However, they have limited use for systems with pronounced mixed conductivity (which is the object under our study), since they provide only average values of the carriers concentration and mobility and do not reflect the contribution of individual types of carriers. More information can be obtained by studying magnetotransport as a function of the magnetic field, in particular quantitative mobility spectrum analysis (QMSA) [4–7]. It allows to obtain densities and mobilities for each carrier present. However, the listed electrophysical methods require significant time for sample preparation, experimentation, and analysis.

Optical methods for determining FCCC are distinguished by the fact that they are express, non-contact and non-destructive. The space locality of the method is determined by the size of the light spot. Such methods include, for example, Raman light scattering [8] and reflectance spectroscopy. The present paper is devoted to the application of the latter. A similar approach was previously applied in relation to heavily doped semiconductor compounds InSb [1], GaAs [2], InAs [3] of *n*-type electrical conductivity. In this paper, the reflection spectra are studied and the technique for determining the FCCC for the tellurium-doped semiconductor compound *n*-GaSb with different carrier concentrations at $T = 295$ K is discussed.

Experiment procedure

n-GaSb samples were obtained by a modified Czochralski method in a combined process [9]. The initial components Ga and Sb (purity 6N), as well as the doping impurity (Te), were placed in a quartz filter crucible, which was installed in the operating crucible of the growth chamber. The synthesis

of the GaSb compound was carried out in a filter crucible at a temperature of $\approx 800^\circ$C in a hydrogen flow atmosphere. After filtering the melt into an operating crucible, the temperature of the melt was reduced to $\approx 714^\circ$C. The single crystal was grown on a seed oriented in the crystallographic direction [100]. The grown single crystal was annealed in the heater zone according to a special thermal condition selected experimentally.

Control plates for measuring electrical parameters and reflection spectra were cut from the top and bottom of the cylindrical part of the single-crystal. The plates were ground using M14 powder and etched in a polishing solution to remove the damaged layer. Samples of approximately square shape with linear dimensions of 10–15 mm were cut from the plates; the thickness of the samples, d, varied within 0.45–2.04 mm (table).

Reflectance spectra R were measured for an incident angle close to the normal. First, they were studied using a Tensor 27 Fourier spectrometer (working wavenumber range $\nu > 340\,\text{cm}^{-1}$). It has been shown that the reflectance in the low-frequency area of the spectrum is highly sensitive to the FCCC of the sample. However, since the frequency of the IR active phonon GsSb did not fall within the operating range of the device, research in the lower frequency area turned out to be important. Subsequently, reflection spectra were measured using a BRUKER IFS66 v/s vacuum Fourier spectrometer in a wide spectral range from 50 to 7500 cm^{-1} at an radiation incident angle close to normal (13°), in two steps: in the far IR spectrum area from 50 to 550 cm^{-1} and in the mid-IR area from 450 to 7500 cm^{-1}. The spectral resolution was 4 cm^{-1}. The source of radiation in both cases was a globar. In the long-wavelength spectral region, a mylar beamsplitter with a coating of germanium and a pyroelectric detector based on DLATGS (deuterated triglycine sulfate with an admixture of L–α-alanine) were used; KBr beam splitter and pyroelectric detector based on DTGS (deuterated triglycine sulfate) were used in short-wavelength area. Next, two spectral regions were merged to obtain a single spectrum over a wide spectral range.

Electrophysical measurements were carried out using traditional four-contact geometry (Van der Pauw method). The contacts were soldered at the corners onto the flat surface of the sample; Indium was used as a contact material. A holder with two samples attached to it on opposite sides was placed in the gap between the poles of the electromagnet. Electrical resistivity was measured in the absence of a magnetic field, and the Hall coefficient was measured in a magnetic field with induction $B = 0.5\,\text{T}$ at a current through the sample of 200 mA.

Experimental results and discussion

Figure 1 shows the reflectance spectra in the far-IR region for four samples with different values of the FCCC. For comparison, we also show the reflection spectrum

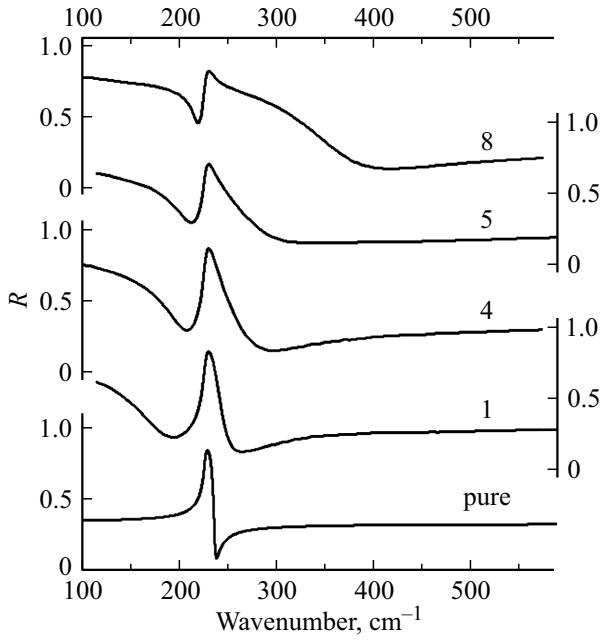

Figure 1. Reflectance spectra for four *n*-GaSb samples compared to the spectrum of a nominally pure GaSb sample. Sample numbers are indicated on the curves, see the Table. FCCC increases upward.

for a nominally pure GaSb single crystal, which has one feature associated with the presence of a single IR active TO phonon with a frequency near 227 cm^{-1}. For all tellurium-doped samples, the reflectance spectrum exhibits an increase in the reflectance at low frequencies or the so-called Drude „tail“, associated with the presence of free charge carriers. An increase in FCCC leads to the advancement of the „tail “ to higher frequencies.

When the phonon frequency is below the frequency of plasma oscillations, it is no longer possible to speak of pure vibrations of the crystal lattice. Two coupled plasmon-phonon modes appear, ν_+ and ν_- [10,11]. In addition, an inversion of TO and LO frequencies occurs (see, for example, [12]). The shape of the phonon becomes „mirror“ symmetrical with respect to the frequency axis (compare the spectra of samples 8 and pure in Fig. 1).

The spectral dependences of the reflectance $R(\nu)$ were modeled using dispersion analysis. The reflection spectrum was calculated using known relations, taking into account the angle of incidence 13°. In this case, the complex dielectric permittivity $\varepsilon(\nu)$ of the sample at frequency ν was described by the sum of the contributions of electronic transitions (ε_∞), the only harmonic (Lorentz) oscillator for GaSb, and a plasmon (Drude formula):

$$\varepsilon(\omega) = \varepsilon_\infty + \frac{S_1^2}{\nu_1^2 - \nu^2 + i\gamma_1\nu} + \frac{\nu_p^2}{-\nu^2 - i\gamma_p\nu}, \qquad (1)$$

where ε_∞ — high-frequency dielectric constant, ν_1 — frequency of the Lorentz oscillator (phonon), S_1 — oscillator

Description of the samples and their characteristics: number, thickness d, resistivity ρ, Hall coefficient modulus $|R_H|$, electron concentration in the Γ-valley n_1 and in the L-valley n_2 and dimensionless parameter b

№ .	d, mm	ρ, Ω·cm	$\lvert R_H\rvert$, cm^3/C	$\nu+$, cm^{-1}	n_1, cm^{-3}	n_2, cm^{-3}	$b = \mu_1/\mu_2$
1	0.96	$3.45 \cdot 10^{-3}$	8.17	260	$3.71 \cdot 10^{17}$	$5.31 \cdot 10^{17}$	2.3
2	0.66	$4.61 \cdot 10^{-3}$	13.8	265	$3.90 \cdot 10^{17}$	$5.64 \cdot 10^{17}$	18
3	0.45	$4.56 \cdot 10^{-3}$	13.8	268	$4.02 \cdot 10^{17}$	$5.85 \cdot 10^{17}$	23
4	0.94	$3.16 \cdot 10^{-3}$	7.74	295	$5.07 \cdot 10^{17}$	$7.91 \cdot 10^{17}$	7.1
5	0.51	$3.04 \cdot 10^{-3}$	8.10	316	$5.90 \cdot 10^{17}$	$9.78 \cdot 10^{17}$	11
6	1.42	$2.56 \cdot 10^{-3}$	5.64	348	$7.15 \cdot 10^{17}$	$1.31 \cdot 10^{18}$	7
7	0.51	$2.88 \cdot 10^{-3}$	6.94	357	$7.50 \cdot 10^{17}$	$1.41 \cdot 10^{18}$	19
8	1.36	$2.32 \cdot 10^{-3}$	6.13	395	$8.98 \cdot 10^{17}$	$1.89 \cdot 10^{18}$	32
9	2.04	$1.71 \cdot 10^{-3}$	4.46	427	$1.02 \cdot 10^{18}$	$2.34 \cdot 10^{18}$	14
10	1.71	$1.73 \cdot 10^{-3}$	4.38	440	$1.08 \cdot 10^{18}$	$2.55 \cdot 10^{18}$	15

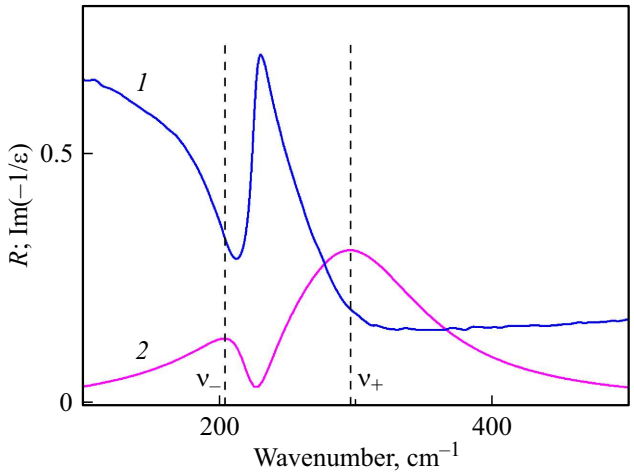

Figure 2. The reflectance spectrum of the sample № 4 (*1*) (see the table) and the loss function (*2*). Vertical dashed lines indicate the characteristic wave numbers $\nu+$ and $\nu-$.

strength, γ_1 — its damping, ν_p — plasma frequency, γ_p — plasmon damping.

The dispersion analysis method is standard for determining experimental optical parameters [15–17]. To simulate the reflectance spectra, the SCOUT [18,19] and RefFit [20] programs were used. The frequency dependence of the reflectance was calculated and compared with experiment. Then the parameters ε_∞, ν_1, S_1, γ_1, ν_p an γ_p were optimized by minimizing the difference between the experimental and calculated spectra. After this, the frequency dependences of the real $\varepsilon_1(\nu)$ and imaginary $\varepsilon_2(\nu)$ parts of the complex dielectric constant $\varepsilon = \varepsilon_2 + i\varepsilon_2$ were calculated and the so-called „loss function“ was constructed:

$$f = \mathrm{Im}(-1/\varepsilon) = \frac{\varepsilon_2}{\varepsilon_1^2 + \varepsilon_2^2}. \qquad (2)$$

It is known that the maximum of the loss function in the limit of small attenuation corresponds to the LO frequency of the corresponding optical mode for nonmetals [21].

Figure 2 shows a typical reflection spectrum (sample № 4, curve *1*; see the table) and the loss function $f(\nu)$ calculated in the manner described above (curve *2*). It can be seen that the loss function has a characteristic form with two wide maxima: the left (low-frequency) is weakly expressed, and the right (high-frequency) is more prominent. The maxima correspond to the wavenumber values corresponding to the frequencies of mixed plasmon-phonon modes: low-frequency ν_- and high-frequency ν_+ ones (for the sample under consideration $\nu_+ = 295\,\mathrm{cm}^{-1}$). The low-frequency plasmon-phonon mode ν_- in the spectral range of interest is not suitable for calculating the value of the FCCC. This mode is determined mainly by the LO phonon, i.e. elastic properties of the crystal lattice, practically independent of the concentration of free charge carriers. To determine the concentration of conduction electrons, the high-frequency value ν_+ is used.

It should be borne in mind that in the *n*-GaSb material at $T = 295\,\mathrm{K}$ there are two types of electrons: light electrons (they are concentrated in the Γ-valley of the conduction band) and heavy electrons, concentrated in the L-valley. The latter is located 85 meV upward in energy from the bottom of the conduction band at the Γ-point [22]; in fractions of kT it will be 3.35 (k — Boltzmann constant; for $T = 295\,\mathrm{K}$, $kT = 25.4\,\mathrm{meV}$).

The electron concentration n_1 in the Γ-valley, which is described by the Kane dispersion law [23], can be calculated using the formula

$$n_1 = \frac{\sqrt{3}}{2\sqrt{2}\pi^2} \frac{(kTE_g)^{3/2}}{P_{cv}^3} {}^0L_0^{3/2}(\eta, \beta). \qquad (3)$$

For the effective mass of electrons m_1 in the Γ-valley, the relation is valid [24]

$$\frac{m_1}{m_0} = \frac{3\hbar^2 E_g}{4P_{cv}^2 m_0} \frac{{}^0L_0^{3/2}(\eta, \beta)}{{}^0L_{-1}^{3/2}(\eta, \beta)}. \qquad (4)$$

In formulas (3) and (4) the following notations are used: $\hbar = \frac{h}{2\pi}$ —reduced Planck's constant; P_{cv} — matrix element of interaction between the valence band and the conduction

band at the point Γ; m_0 is free electron mass; E_g is band gap width. Formulas (3) and (4) use two-parameter Fermi integrals:

$$^{m}L_k^n(\eta,\beta)=\int_0^\infty\left(-\frac{\partial f_0}{\partial x}\right)\frac{x^m(x+\beta x^2)^n}{(1+2\beta x)^k}\,dx, \qquad (5)$$

where $f_0=[1+\exp(x-\eta)]^{-1}$ is Fermi function.

The dimensionless parameter $\eta=E_F/kT$ (reduced Fermi level) is counted upward from the bottom of the conduction band at the Γ-point of the Brillouin zone; $\beta=kT/E_g$ — dimensionless parameter characterizing the nonparabolicity of the conduction band in the Γ-valley (for GaSb at $T=295\,\mathrm{K}$, $\beta=0.0349$).

The electron concentration n_2 in the L-valley (it consists of four identical ellipsoids and is considered to be parabolic) is described by the relation [25]

$$n_2=M\,\frac{8\pi}{3h^3}\,(2m_d^{(1)}kT)^{3/2}F_{3/2}(\eta-3.35). \qquad (6)$$

Here $M=4$ is the number of ellipsoids in the L valley; $m_d^{(1)}$ is an effective mass of the density of states per one ellipsoid; $F_{3/2}(\eta-3.35)$ is one-parameter Fermi integral (the integral $^0L_0^{3/2}(\eta;\beta)$ goes into the integral $F_{3/2}(\eta)$ at $\beta=0$, i.e. in the case when the nonparabolicity of the band can be neglected. In the argument of the integral in formula (5) it is not η, but $(\eta-3.35)$ since the L-valley is separated from the Γ-valley by $3.35\,kT$ (see above).

For the effective mass of the density of states in the L-valley of the conduction band, the relation is valid (per one ellipsoid) [25]

$$m_d^{(1)}=(m_t^2\times m_l)^{1/3}=m_t\times K_1^{1/3}=0.2257m_0, \qquad (7)$$

where $K_1=\frac{m_l}{m_t}$ is ellipsoid anisotropy coefficient; m_l and m_t are longitudinal and transverse effective masses, respectively ($K_1=8.64$; $m_t=0.11\ m_0$ [22]).

The effective mass m_2 of conductivity in the L-valley is determined from the condition [25]

$$\frac{3}{m_2}=\frac{2}{m_t}+\frac{1}{m_l}. \qquad (8)$$

In accordance with formula (8) $m_2=0.156m_0$. Calculations using formula (4) show that in the range of $-4\le\eta\le4$ values, the effective mass of electrons in the Γ-valley varies within $0.0645-0.0745m_0$ (this is due to the nonparabolicity of the Γ-valley of the conduction band). It can be seen that m_2 is more than twice as large as m_1.

For the plasmon frequency ω_p the following relation is valid (contributions from Γ- and L-valleys are considered additive) [26]

$$\omega_p^2=\frac{4\pi e^2}{\varepsilon_\infty m_0}\left[\frac{n_1}{m_1/m_0}+\frac{n_2}{m_2/m_0}\right]. \qquad (9)$$

Here e is electron charge; ε_∞ is high frequency dielectric constant.

In terms of wave numbers, for the wave number ν_p corresponding to the plasma frequency, we obtain

$$\nu_p(\mathrm{cm}^{-1})=7.675\cdot10^{-8}\sqrt{\frac{n_1}{m_1/m_0}+\frac{n_2}{0.156}}. \qquad (10)$$

If we neglect the damping of plasmons and LO phonons, then the dielectric constant $\varepsilon(\omega)$ can be represented as a real function of frequency ω:

$$\varepsilon(\omega)=\varepsilon_\infty\left[1-\left(\frac{\omega_p}{\omega}\right)^2\right]+(\varepsilon_0-\varepsilon_\infty)\left[1-\frac{\varepsilon_0}{\varepsilon_\infty}\left(\frac{\omega}{\omega_{\mathrm{LO}}}\right)^2\right]^{-1}. \qquad (11)$$

Here ε_0 — static dielectric constant, ω_{LO} — frequency of longitudinal optical phonon. The first term in formula (11) describes the contribution from conduction electrons, and the second — from the crystal lattice. Equating $\varepsilon(\omega)$ to zero and passing to wave numbers, after solving the biquadratic equation we obtain the values of wave numbers ν_+ and ν_- corresponding to the frequencies of the mixed plasmon-phonon modes ω_+ and ω_-:

$$\nu_\pm^2=\frac{1}{2}\left[(\nu_p^2+\nu_{\mathrm{LO}}^2)\pm\sqrt{(\nu_p^2+\nu_{\mathrm{LO}}^2)^2-4\,\frac{\varepsilon_\infty}{\varepsilon_0}\,\nu_p^2\nu_{\mathrm{LO}}^2}\right]. \qquad (12)$$

Here ν_{LO} is wave number corresponding to the frequency of the longitudinal optical phonon.

The following values of the parameters included in the above formulas were used in the calculations:

– band gap width $E_g=0.728\,\mathrm{eV}$ [22];

– high-frequency dielectric constant $\varepsilon_\infty=15.2$ [27];

– static dielectric constant $\varepsilon_0=16.4$ [27];

– matrix element of interaction between valence and conduction bands in the Γ valley $P_{cv}=8.7\cdot10^{-8}\,\mathrm{eV\cdot cm}$ [27];

– wave number corresponding to the frequency of the longitudinal optical phonon, $\nu_{\mathrm{LO}}=240\,\mathrm{cm}^{-1}$ [27];

– reduced Fermi level $\eta=E_{\mathrm{F}}/kT$ (from −4 to +4).

To determine the electron concentration value, the following algorithm was used:

1) the value of the reduced Fermi level was specified;

2) using formulas (3), (4), (6), the values of the electron concentrations n_1 and n_2, as well as the values of the reduced effective mass of electrons in the Γ valley, were calculated;

3) using formula (10) the corresponding value ν_p was calculated;

4) using formula (12), the values of ν_+ and ν_- were calculated;

5) a different value of the parameter $\eta=E_{\mathrm{F}}/kT$ was set, and operations were repeated according to clauses (1)−(4) in the range from −4 to +4;

6) as a result, two calibration dependencies were constructed: $n_1(\nu_+)$ and $n_2(\nu_+)$ (Fig. 3), allowing the known value of ν_+ to determine the values of electron concentrations n_1 and n_2.

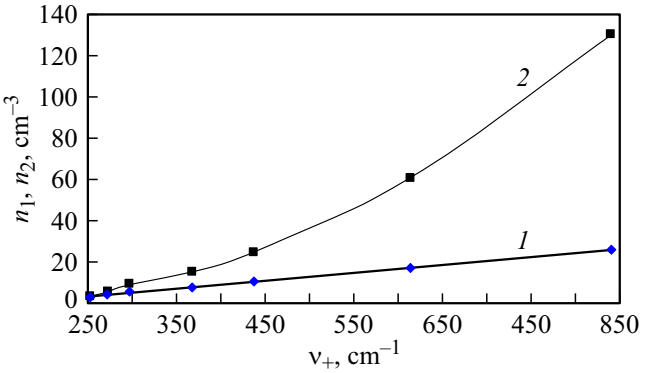

Figure 3. Calculated calibration dependences $n_1(\nu+)$ (*1*) and $n_2(\nu+)$ (*2*).

Let us note that the parameters used in the calculations are in common use. Nevertheless, to use this technique, for example, in production, it is required to scale these curves within small limits according to the measurements of reference samples, as is customary in spectral analysis [28]. The preparation of such samples should rely on a reliable method, which appears to be the QMSA mentioned in the introduction.

The first dependence is linear, the second is — quadratic:

$$n_1 = 3.908 \cdot 10^{15}\nu_+ - 6.454 \cdot 10^{17}, \quad (13)$$

$$n_2 = 2.591 \cdot 10^{13}(\nu_+)^2 - 6.944 \cdot 10^{15}\nu_+ + 5.850 \cdot 10^{17}. \quad (14)$$

In formulas (13) and (14), the values n_1 and n_2 are taken in cm^{-3}, and the values ν_+ — in cm^{-1}.

Let us note that the error in determining n_1 and n_2 will be maximum in the region of low frequencies, when the values of ν_+ are close to the wave number of the longitudinal optical phonon ($\nu_{LO} = 240\,\text{cm}^{-1}$ [27]). Estimates show that at $\nu \geq 300\,\text{cm}^{-1}$ the relative error in determining n_1 and n_2 does not exceed $\pm 10\%$, decreasing with increasing values ν_+.

Thus, having processed the experimental reflection spectrum of the sample under study and determined the value of ν_+ (see above), it is now easy to calculate the values of n_1 and n_2 using formulas (13) and (14).

As mentioned above, in the material under consideration at $T = 295\,\text{K}$ there are electrons of two types: „light“ in the Γ-valley and „heavy“ in the L-valley, and, as calculations show (Fig. 3), the concentration of the latter noticeably predominates. Detailed calculations of the statistics of free charge carriers in *n*-GaSb at $T = 295\,\text{K}$ and $T = 77\,\text{K}$ are presented in paper [29]. At $T = 295\,\text{K}$ it is inappropriate to use the commonly used simple formulas to calculate the concentration n and mobility μ_n of electrons:

$$n = \frac{1}{|R_H| \times e}, \quad (15)$$

$$\mu_n = \frac{|R_H|}{\rho}. \quad (16)$$

Here R_H is Hall coefficient, ρ is electrical resistivity.

The formula for the modulus of the Hall coefficient in weak magnetic fields in the presence of conduction electrons of two types takes the form

$$|R_H| = \frac{1}{e}\frac{(n_1\mu_1^2 + n_2\mu_2^2)}{(n_1\mu_1 + n_2\mu_2)^2}, \quad (17)$$

where μ_1 and μ_2 are respectively, the mobility of electrons in the Γ and L valleys of the conduction band.

By introducing the dimensionless parameter $b = \mu_1/\mu_2$, formula (17) can be transformed to the form

$$|R_H| = \frac{1}{e}\frac{(n_1 b^2 + n_2)}{(n_1 b + n_2)^2}, \quad (18)$$

Since the value of parameter b is not known in advance, the values of n_1 and n_2 cannot be determined. However, if we take n_1 and n_2 from optical data, then substituting them into formula (18), using the value R_H known from electrical measurements, we can calculate the value of the parameter b.

The table presents the parameters of the studied samples and the results of electrophysical and optical measurements performed at room temperature. The samples are arranged in ascending order of ν_+ values. The random relative error in determining the values of ρ is 3%, in determining the values of R — 6%. The estimated error in determining the parameter value b does not exceed 20%.

The table shows that over the entire concentration range $n_2 > n_1$, and this difference increases as ν_+ increases, i.e. conduction electrons are concentrated mainly in the L-valley. The b values vary from 2.3 (sample № 1) to 3.2 (sample № 8). Let us note that there is no correlation between the values of the parameter b and the values of ν_+.

It should be noted that the determination of the parameter b value was attempted earlier [30–33], but all of them were based on an analysis of the dependences of electrical parameters on temperature and pressure. Meanwhile, assumptions were introduced into the theoretical models, used to describe the observed experimental data, that can hardly be considered justified. Thus, in papers [30,31] it is assumed that the total concentration of electrons in the Γ- and L-valleys of $n = n_1 + n_2$ remains constant over a wide temperature range and is exactly equal to the concentration of introduced tellurium atoms, which are considered to be completely ionized. The authors do not provide experimental data confirming this dubious assumption. As a result, the value $b = 6$ was obtained (the same for a wide temperature range), which can hardly be considered reliable.

On the contrary, the authors of the paper [32] emphasize that the value of the total electron concentration n depends on temperature and that the value of the parameter b varies within 5–21; in the paper [33] the value $b = 16.7$ is given.

Thus, it can be argued that the method of determining the parameter b described in this paper has not been used by anyone so far and is used by us for the first time.

It is also surprising that, while recognizing the validity of Kane's model for the Γ-valley, the authors of a number of papers [31–35] for some reason use in their calculations the values of the effective masses at the bottom of the Γ valley from $0.039m_0$ [34] to $0.052m_0$ [33]; the most commonly used value is $0.047m_0$, first obtained in the paper [35] for the temperatures $T = 1.5\,\mathrm{K}$ and $T = 4.2\,\mathrm{K}$. At the same time, direct calculation using formula (4) shows that at zero temperature the effective mass of the electron at the bottom of the Γ valley is equal to $0.055m_0$ (which practically coincides with the upper value available in the literature for the effective mass $0.052m_0$ [33]), and with $T = 295$,K in the range of values $-4 \le \eta \le +4$ m_1 changes within the limits of $(0.0645-0.0745)m_0$ (see above), which is significantly greater than the values given in the papers [30–35]. The entire statistics of electrons in the Γ valley changes accordingly.

It was already mentioned above that the effective mass of „heavy" electrons is more than twice the same value for „light" electrons. If the mobility ratio were determined only by the effective mass ratio, the value of the parameter b would be the same. However, as can be seen from the table, the values of the parameter b are noticeably larger. Since $\mu = e\tau/m$ (τ is the average relaxation time of an electron with respect to quasi-momentum), we have to assume that the difference in the mobilities of light electrons and heavy electrons is due to the difference in the values of τ, i.e. in electron scattering mechanisms [33,36].

In the Ref. [37], the electron concentrations n_1 and n_2 were determined in two ways: from Raman light scattering (RS) and from electrophysical measurement data. Let us note that when calculating the values of n_1, we used not two-parameter Fermi integrals, which are used in Kane theory [6,7], but one-parameter ones, which, in our opinion, is incorrect. As a result, values in the range $5-11$ were obtained for parameter b. It was also shown that the difference between the Hall and RS values of the total electron concentration $n = n_1 + n_2$ changes monotonically with increasing doping level from -16% to $+24\%$ [35].

It is also required to evaluate whether the condition of weak magnetic fields is satisfied for the samples we studied: $\mu^2B^2 \ll 1$. For a crude estimate, we will use formula (16), assuming that the data obtained will relate to light electrons. As can be seen from formula (18), the first term in the sums of both numerator and denominator of the fraction is noticeably larger than the second. As a result, we find that for the samples listed in the table, μ_1 does not exceed $3 \cdot 10^3\,\mathrm{cm}^2/(\mathrm{V{\cdot}s})$. For magnetic field induction $B = 0.5\,\mathrm{T}$ $\mu^2B^2 = 0.0225 \ll 1$, i.e. the condition of a weak magnetic field is satisfied for „light" electrons and even more for „heavy" ones.

Conclusions

1. A method is proposed for separately determining the concentrations of light electrons (n_1) and heavy electrons (n_2) in n-GaSb at $T = 295\,\mathrm{K}$. Calculated calibration dependences have been constructed that allow to determine the values of n_1 and n_2 from the value of the characteristic wave number ν_+ corresponding to the frequency of the high-frequency mixed plasmon-phonon mode.

2. The reflection spectra of n-GaSb samples were measured in the far IR area at room temperature. Using the analysis of the obtained spectra, the values of the characteristic wave number ν_+ were calculated and the values of the electron concentrations n_1 and n_2 were determined.

3. Electrophysical measurements were performed on the same samples using the Van der Pauw method at room temperature. By comparing optical and Hall data, the values of the ratio of mobilities „light" and „heavy" electrons b were determined. This method of determining the value of the parameter b was used for the first time.

Conflict of interest

The authors declare that they have no conflict of interest.

References

[1] I.M. Belova, A.G. Belov, V.E. Kanevskii, A.P. Lysenko. Semiconductors, **52** (15), 1942 (2018). DOI: 10.1134/S1063782618150034
[2] T.G. Yugova, A.G. Belov, V.E. Kanevskii, E.I. Kladova, S.N. Knyazev. Modern Electronic Materials, **6** (3), 85 (2020). DOI: 10.3897/j.moem.6.3.64492
[3] T.G. Yugova, A.G. Belov, V.E. Kanevskii, E.I. Kladova, S.N. Knyazev, I.B. Parfent'eva. Modern Electronic Materials, **7** (3), 79 (2021). DOI: 10.3897/j.moem.7.3.76700
[4] O.V.S.N. Murthy, V. Venkataraman. Phys. Status Solidi C, **6**, 1505 (2009). DOI: 10.1002/pssc.200881539
[5] D.V. Gulyaev, K.S. Zhuravlev, A.K. Bakarov, A.I. Toropov, D.Yu. Protasov, A.K. Gutakovskii, B.Ya. Ber, D.Yu. Kazantsev. J. Phys. D: Appl. Phys., **49** (9), 095108 (2016). DOI: 10.1088/0022-3727/49/9/095108
[6] J. Antoszewski, G. Umana-Membreno, L. Faraone. J. Electron. Mater., **41**, 2816 (2012). DOI: 10.1007/s11664-012-1978-9
[7] I. Vurgaftman, J.R. Meyer, C.A. Hoffman, S. Cho, J.B. Ketterson, L. Faraone, J. Antoszewski, J.R. Lindemuth. J. Electron. Mater., **28**, 548 (1999). DOI: 10.1007/s11664-999-0110-2
[8] J.E. Maslar, W.S. Hurst, C.A. Wang. J. Appl. Phys., **103**, 013502 (2008). DOI: 10.1063/1.2828147
[9] Patent № 2528995 Russian Federation, IPC S30B15/02 (2006.01), C30B15/04 (2006.01), C300B29/40 (2006.01). „Method for producing large single-crystals of gallium antimonide" № 2013118771/05; application 04/24/2013. Publ. 09/20/2014 / Ezhlov V.S., Milvidskaya A.G., Molodtsova E.V., Mezhenny M.V. Applicant JSC „Giredmet", 8 p.
[10] B.B. Varga. Phys. Rev. A, **137**, 1896 (1965). DOI: 10.1103/PhysRev.137.A1896
[11] A.A. Kukharskii. Solid State Commun., **13** (11), 1761 (1973). DOI: 10.1016/0038-1098(73)90724-2.
[12] E.A. Vinogradov. UFN, **190**, 829 (2020) (in Russian). DOI: 10.3367/UFNe.2020.01.038719
[13] V.A. Kizel'. *Otrazheniye sveta* (Nauka, M., 1973). (in Russian)

[14] P. Grosse. *(Svobodnyye elektrony v tverdykh telakh* (Mir, M., 1982) (in Russian).
[15] N. Popova, A.B. Sushkov, S.A. Klimin, E.P. Chukalina, B.Z. Malkin, M. Isobe, Y. Ueda. Phys. Rev. B, **65**, 144303 (2002). DOI: 10.1103/PhysRevB.65.144303
[16] N.N. Novikova, V.A. Yakovlev, S.A. Klimin, T.V. Malin, A.M. Gilinskii, K.S. Zhuravlev. Opt. Spectrosc., **127** (7), 36 (2019). DOI: 10.1134/S0030400X19070208.
[17] S.A. Klimin, A.B. Kuzmenko, M.N. Popova, B.Z. Malkin, I.V. Telegina. Phys. Rev. B, **82**, 174425 (2010). DOI: 10.1103/PhysRevB.82.174425
[18] W. Theiß, Surf. Sci. Rep., **29** (3–4), 91 (1997). DOI: 10.1016/S0167-5729(96)00012-X
[19] M. Krüger, S. Hilbrich, M. Thönissen et al. Opt. Commun., **146**, 309 (1998).
[20] A.B. Kuzmenko. Rev. Sci. Instruments, **76**, 083108 (2005).
[21] E.A. Vinogradov. *Spektroskopiya kolebatel'nykh sostoyaniy kvazidvumernykh poluprovodnikovykh struktur*. Avtoref. dokt. dis. (In-t spektroskopii RAN, Troitsk, 1982). (in Russian).
[22] GaSb — Gallium Antimonide. Band structure and carrier concentration. [Electronic source]. URL: https://www.ioffe.ru/SVA/NSM/Semicond/GaSb/bandstr.html
[23] E.O. Kane. J. Phys. Chem. Solids, **1** (4), 249 (1957). DOI: 10.1016/0022-3697(57)90013-6
[24] Yu.I. Ravich, B.A. Efimova, I.A. Smirnov. *Metody issledovaniya poluprovodnikov v primenenii k khal'kogenidam svintsa PbTe, PbSe, PbS* (Nauka, M., 1968) (in Russian).
[25] B.M. Askerov. *Kineticheskiye effekty v poluprovodnikakh* (Nauka, M., 1970) (in Russian).
[26] Yu.K. Pozhela. *Plazma i tokovyye neustoychivosti v poluprovodnikakh* (Nauka, M., 1977) (in Russian).
[27] O. Madelung. *Physics of III-V Compounds* (Wiley, New York, 1964).
[28] A.N. Zaydel'. *Osnovy spektral'nogo analiza* (Nauka, M., 1965), 324 p. (in Russian).
[29] Yu.N. Parkhomenko, A.G. Belov, E.V. Molodtsova, R.Yu. Kozlov, S.S. Kormilitsina, E.O. Zhuravlev. Modern Electronic Materials, **8** (4), 165 (2022). DOI: 10.3897/j.moem.8.4.100756
[30] A. Sagar. Phys. Rev., **117** (1), 93 (1960). DOI: 10.1103/PhysRev.117.93
[31] A.J. Strauss. Phys. Rev., **121** (4), 1087 (1961). DOI: 10.1103/PhysRev.121.1087
[32] H.B. Harland, J.C. Woolley. Canad. J. Phys., **44** (11), 2715 (1966). DOI: 10.1139/p66-221
[33] W.M. Becker, A.K. Ramdas, H.Y. Fan. J. Appl. Phys., **32** (10), 2094 (1961). DOI: 10.1063/1.1777023
[34] G.R. Johnson, B.C. Cavenett, T.M. Kerr, P.B. Kirby, C.E.C. Wood. Semicond. Sci. Technol., **3** (12), 1157 (1988). DOI: 10.1088/0268-1242/3/12/002
[35] S. Zwerdling, B. Lax, K.J. Button, L.M. Roth. J. Phys. Chem. Sol., **9**, 320 (1959). DOI: 10.1016/0022-3697(59)90109-X
[36] V.W.L. Chin. Solid-State Electronics, **38** (1), 59 (1995). DOI: 10.1016/0038-1101(94)E0063-K
[37] J.E. Maslar, W.S. Hurst, C.A. Wang. J. Appl. Phys., **104** (10), 103521 (2008). DOI: 10.1063/1.3021159

Translated by E.Potapova